

Physical conditions and molecular chemistry of the Central Molecular Zone

This article has been downloaded from IOPscience. Please scroll down to see the full text article.

2006 J. Phys.: Conf. Ser. 54 35

(<http://iopscience.iop.org/1742-6596/54/1/006>)

View [the table of contents for this issue](#), or go to the [journal homepage](#) for more

Download details:

IP Address: 38.107.179.211

The article was downloaded on 13/02/2012 at 06:05

Please note that [terms and conditions apply](#).

Physical conditions and molecular chemistry of the Central Molecular Zone

Nemesio J. Rodríguez-Fernández¹

¹ Observatoire de Bordeaux (L3AB/OASU), CNRS/Université Bordeaux 1, BP 89, 33270 Floirac, France

E-mail: nemesio.rodriquez@obs.u-bordeaux1.fr

Abstract. We discuss the physical conditions of the different kinematical components of the Central Molecular Zone. In particular we compare the properties of the clouds moving with in elongated orbits along the Galactic bar with those of the well-known Galactic center ring (GCR) clouds (Sgr A, Sgr B2,...). We show that all the components contain dense clouds that can withstand the tidal shear. The SiO abundance in the clouds with non-circular velocities is high ($\sim 10^{-8}$), in perfect agreement with that of the GCR clouds. We discuss the role of the UV radiation and C-shocks in the heating of the neutral gas and the high abundances of some molecules like SiO. The SiO emission in the clouds moving in elongated trajectories is probably due to the cloud collisions expected in the inner regions of a bar.

1. Morphology and kinematics of the Central Molecular Zone

Figure 1 shows a schematic view of the longitude-velocity diagram (hereafter *lv*-diagram) of the Galactic center (GC) as observed in CO [3, 7, 24, 5]. The Central Molecular Zone (CMZ) is the region from $l = -1^\circ$ to $l = 1.5^\circ$ (the $l = 1.3^\circ$ -complex) [23]. The important cloud complexes from Sgr C to Sgr D are located approximately along a line passing through the origin. Therefore, in a face-on view of the Galactic center the Sgr complexes would be located in a circular ring (Fig. 2). Hereafter, we refer to this structure as the Galactic center ring (GCR). However, the GCR clouds and the $l = 1.3^\circ$ -complex are not the only cloud components in the GC. The *lv*-diagram also exhibits many structures corresponding to clouds moving in non-circular trajectories like the Clump 2, the Connecting Arm, or the structures that we have labeled as J, K, L, M and N (Fig. 1). The easiest explanation for the non-circular trajectories is the gas response to a bar potential [4, 8].

Numerical simulations of the gas dynamics in the inner region of barred galaxies [1, 8] show that the gas follows elongated orbits along the bar major axis until the contact point where these gas clouds interact with the clouds in the nuclear disk (GCR). The gas is then sprayed and it collides with the material on the opposite side of the bar major axis giving rise to shocks in the molecular cloud component and to the characteristic dust lanes that are observed near the leading edges of the bars in external galaxies like NGC 1300, NGC 1530 or NGC 6951. In the GC, the near-side dust lane has been identified as the Connecting Arm [8]. The structure K, which seems to be linked to the Connecting Arm at $l \sim 3^\circ$ (Fig. 1), represents gas clouds that move in the decelerating section of elongated orbits, i.e, gas that does not fall in the nuclear ring at the first passage around the interaction region (see Fig. 2). The structure J has nearly the

same inclination as that of the Connecting Arm (Fig. 1), and it could be a kind of small dust lane, but in contrast with the Connecting Arm and the structure K, the gas in the structure J will easily interact with the material of the nuclear disk in the area of the $l = 1.3^\circ$ -complex (see Fig. 2). Thus, the $l = 1.3^\circ$ -complex would be the contact point of the dust lane and the GCR as proposed by previous works [11, 8]. The clump at $l = 5^\circ$ and the Clump 2 are gas clouds that are about to enter the dust lane shock. The lv -diagram at $l < 0$ is more difficult to interpret. Due to perspective effects the far side dust lane is elongated along the line of sight and thus it is a vertical structure in the lv -diagram close to the extremity of the nuclear ring (see Fig. 23 of reference [8]). Therefore, the lv -diagram is not expected to be symmetric. The structure M would be part of the gas spray due to the interaction of the far-side dust lane and the GCR.

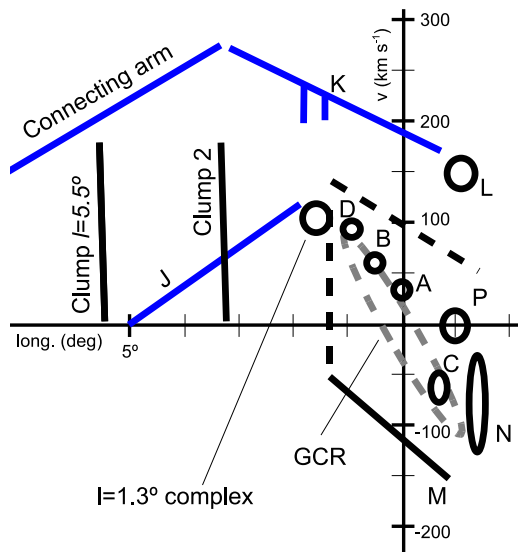


Figure 1. Schema illustrating the main kinematical structures in the longitude-velocity diagram of the inner degrees of the Galaxy. The labels A to D stand for Sgr A to Sgr D complexes. See the text for an explanation of the other labels.

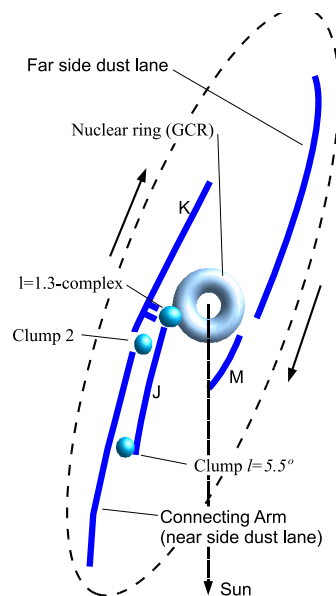


Figure 2. Schema of a plausible face on view of the Galactic center.

2. Physical conditions and molecular chemistry

2.1. The Galactic center ring

The physical conditions of the neutral gas in the GC have been studied by observing high density tracers like CS [3, 39] or HCN [13] and by multi-level studies of NH_3 [11], H_2 [28, 30] or CO [34, 16]. These works, among others, have shown that the clouds in the GCR and the $l = 1.3^\circ$ -complex are dense (10^4 cm^{-3}) and warm (up to $\sim 150 \text{ K}$). Fine structure lines observations of several elements in different ionization stages have allowed to study in detail the heating mechanisms of the warm molecular gas [30, 31]. The CMZ is permeated by hot star radiation ($\sim 35000 \text{ K}$) like that present in the vicinity of the Arches and the Quintuplet clusters in the Radio Arc region [29]. This radiation ionizes the surface of the molecular clouds [31]. In the interface of the ionized gas and the well-shielded molecular gas there are mainly neutral photo-dissociation regions (PDRs). The intensity of the main cooling lines ($[\text{CII}] 158 \mu\text{m}$, $[\text{OI}] 63 \mu\text{m}$) and the temperature of the warm H_2 ($\sim 150 \text{ K}$) are in perfect agreement with PDR models with an incident far-UV field 1000 times higher than the local interstellar

radiation field and a density of 1000 cm^{-3} [30]. The far-infrared continuum emission from the warm ($\sim 35 \text{ K}$) dust component also agrees with this scenario of heating in PDRs. However, only a small fraction (10-30 %) of the total column density of warm H_2 can be explained by the PDR models [30]. One possibility to explain the heating of the large quantity of molecular gas measured in the GC clouds is the presence of magneto-hydrodynamic continuous (C) shocks. An important parameter in C-shock models is $b = B/\sqrt{n}$, where B is the intensity of the magnetic field expressed in μG and n is the hydrogen density in cm^{-3} . We have compared the measured intensities of the lowest H_2 pure-rotational lines with the C-shock models by Pineau des Forets and collaborators [6]. Figure 3 shows that C-shocks models with $b = 10$ (for instance $B = 300 \mu\text{G}$ and $n = 1000 \text{ cm}^{-3}$) can explain the observed intensity of the H_2 lines in the GC (see also [30]).

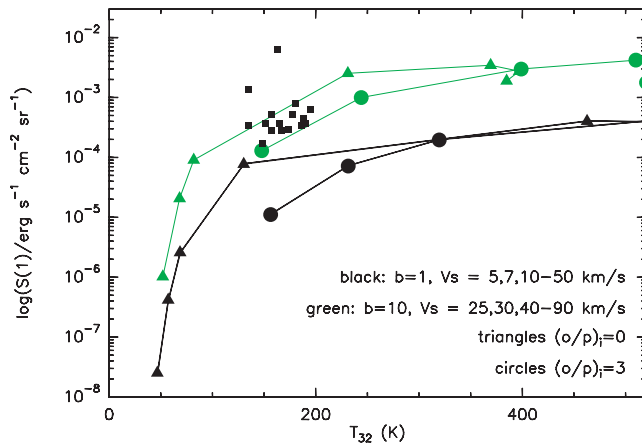


Figure 3. C-shocks model predictions for the intensity of the H_2 S(1) line as a function of the excitation temperature derived from the S(1) and the S(0) lines for different shock velocities (v_s), $b = B(\mu\text{G})/\sqrt{n(\text{cm}^{-3})}$ (black lines: 1, light lines: 10), and initial ortho/para ratio (triangles: 0, circles: 3). The solid squares represent the intensity measured for the GC clouds [28]

The GCR clouds also present widespread emission and high abundances of molecules like SiO, SO, CH_3OH , $\text{C}_2\text{H}_5\text{OH}$ and other organic molecules that have been ejected from the dust grains. The abundances of these molecules also imply the presence of shocks in the CMZ.

(i) The quantity of warm NH_3 measured in the GC clouds [11] cannot be explained by thermal evaporation of the grain mantles. First, the dust temperature is lower than 35 K [30]. Second, this molecule is easily dissociated in the presence of UV radiation. Taking into account the photo-dissociation rates and the NH_3 abundances in the CMZ one derives that a few 10^{22} cm^{-2} of H_2 should be heated every $\sim 10 \text{ yr}$, which is not realistic [30]. The easiest way to explain the NH_3 abundance in gas phase is grain mantle erosion by mechanical processes.

(ii) The abundance of CH_3OH , $\text{C}_2\text{H}_5\text{OH}$ and other complex organic molecules is high in the CMZ clouds that are not associated with thermal continuum sources [21, 14, 25]. In contrast, their abundances decrease by more than a factor 10 in the clouds located in the vicinity of thermal continuum sources [21, 25].

(iii) The SiO is particularly interesting since the abundance of this molecule shows extreme variations in the Galaxy from $< 5 \cdot 10^{-12}$ in dark clouds [43] to $10^{-11} - 10^{-10}$ in diffuse translucent clouds and in spiral arms clouds [9, 15]. The SiO abundance is also very low ($\sim 10^{-11}$) in PDRs [35]). In contrast, the SiO abundance in shocked regions associated to star formation is $\sim 10^{-8}$ [17, 2]. In these regions, the Si and SiO abundances in the gas phase are increased by the processing of the dust grains by shock waves [36]. The SiO abundances in GCR clouds are $\sim 10^{-8}$ [18, 11], as high as those found in shocked regions.

Shocks can explain the molecular chemistry and the high temperatures of the neutral gas in the GCR, and the $l = 1.3^\circ$ -complex. However the origin of the shocks is not clear. For instance, it could be related to the interaction of evolved massive stars with the surrounding interstellar medium [20]. Alternatively, cloud-cloud collisions induced by the large scale dynamics of the

Galaxy could also play a role [42, 11, 21, 33, 27, 30]. Perhaps the best evidence of the effect of the Galactic dynamics on the physical conditions of the GC molecular clouds is the high SiO abundance measured in the $l = 1.3^\circ$ -complex [11], since this region seems to be the interaction region between gas moving in elongated orbits along the bar and the gas moving in circular orbits in the GCR [8].

2.2. Clouds with non-circular velocities

Different energetic phenomena are taking place in the inner regions of the GC (birth and death of massive stars, energetic radiation, shocks,...) making it very complex to interpret the observations of the GCR clouds. The study of less complex regions can give us important hints on the origin of the physical conditions of the CMZ. The clouds with non-circular velocities do not present signs of star-formation [24, 32]. Furthermore, as discussed in Sect. 1, their physical conditions can be affected by the global gas dynamics. However, in contrast to the GCR cloud complexes, the physical conditions of the gas with non-circular velocities that constitute the characteristic shape of the lv -diagram are not well-known. The few large scale maps that have been used to study the physical conditions of the ensemble of the GC molecular gas show that the CO(2-1) to CO(1-0) ratio is rather constant (~ 1) in the GC clouds (including Clump 2) [24, 34]. A few clouds of the upper-right corner of the lv -diagram have been observed in SiO and NH₃ [12, 11] and in H₂ and fine structure lines [30]. Their densities and temperatures are similar to the GCR clouds.

Recently, it has been presented the results of a survey of CS(2-1) and SiO(2-1) in 161 clouds belonging to all the kinematical components of the Galactic center in the longitude range $3.5^\circ > l > -1.5^\circ$ [32]. The results are displayed graphically in Fig. 4. Blue triangles and bars represent the peak velocity and the full width at half maximum (FWHM) of the sources detected in CS. Black points and bars show the peak velocity and FWHM of the sources detected in CS and SiO.

2.2.1. Density

In addition to the GCR and the $l = 1.3^\circ$ -complex, CS emission is detected in all the kinematical structures of the GC lv -diagram (Fig 4) like the faint structures that constitute the upper and lower edges of the lv -diagram (K, M, R), including the vertical appendix of the component K at $l \sim 1.7^\circ$, which can be the signature of mass transfer from the elongated orbits to the GCR [8] or the clouds in the right edge of the lv -diagram (L, N, P) and those in the structure J. These observations demonstrate that there are dense CS-emitting clouds ($n > 10^4 \text{ cm}^{-3}$) in all the kinematical components seen in the CO lv -diagram and not only in the GCR and the $l = 1.3^\circ$ -complex clouds detected by previous works [3]. The critical density to withstand the tidal shear at the galactocentric radius of the clouds with non-circular velocities is $\sim 10^3 \text{ cm}^{-3}$ [38]. Therefore, the CS clouds in non-circular orbits are gravitationally bound and the dust lanes do not contain diffuse gas only [32]. However, there are no signs of star formation in the dust lanes. Indeed, the lack of star formation along the dust lanes is common in the observations of other barred galaxies, where there is star formation in the nuclear ring and at the extremities of the bar, but there are no signs of star formation in the dust lanes along the bar [40, 26, 37]. The inhibition of the star formation can be an effect of the high velocities, relative to the gas in the dust lanes, of the dense clouds whose orbits intersect the dust lanes [40]. These velocities are much higher in barred than in normal galaxies. The high velocity can cause a quick compression of the clouds followed by a rapid expansion which disperses the majority of the cloud. This mechanism has also been invoked to explain the observations of NGC 1530 [26] and it could also inhibit the star formation in the gas with non-circular velocities in the GC [32].

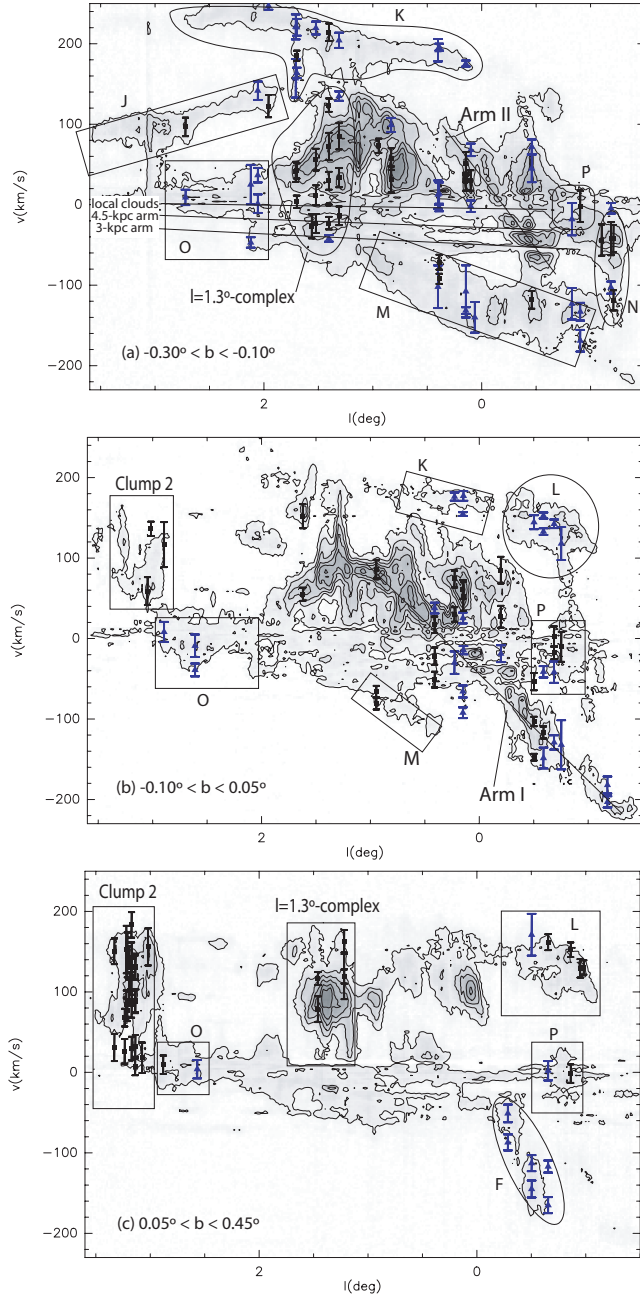


Figure 4. In grey-levels and contours we show the longitude-velocity diagram obtained with the CO(1-0) data by [3] at different latitude ranges. We also indicate the different kinematical features discussed in this paper (note that not all the features that are seen in different panels are labeled in all of them). Triangles and bars represent the peak velocity and the full width at half maximum (FWHM) of the sources detected in CS. Black points and bars show the peak velocity and FWHM of the sources that have been detected in CS and SiO.

2.2.2. SiO abundances SiO(2-1) emission has also been detected in at least a few clouds of all the kinematical components [32]. The SiO(2-1) line has been detected in all the observed clouds of the $l = 1.3^\circ$ -complex and Clump 2. The SiO line has also been detected in two clouds of the component K: one cloud near the CO maximum at $l \sim 1.4$ and one cloud in the vertical appendix at $l \sim 1.7^\circ$. SiO emission has also been detected in the lower edge (component M) and the negative longitude extremity of the lv -diagram (components P and N, including a few clouds with different velocities along the structure N) as well as towards several positions in the structures J and L. In most of the clouds where the SiO line has not been detected the CS is indeed rather weak and the upper limits to the SiO/CS line ratio are not significant.

The SiO abundances in the clouds with non-circular velocities with detected SiO are $(0.5-8) \cdot 10^{-9}$ [32], including those in the structures K and M. These abundances are in agreement

with those measured in the GCR and the $l = 1.3^\circ$ -complex [11, 18, 19]. For one source in the Sgr B2 area ($l = 0.83^\circ$, $b = -0.18^\circ$, $v = 57 \text{ km s}^{-1}$) and two in the feature P we have even measured a SiO abundance of $\sim 10^{-8}$, which is comparable to the highest abundances derived in the $l = 1.3^\circ$ -complex [11].

The high SiO abundances measured in the GC clouds with non-circular velocities should be due to the strong shocks that created the dust lanes themselves. This scenario has also been proposed to interpret the detection of HNC, CH₃OH and SiO emission along the bar of IC 342 [22, 41].

3. Conclusions

We have compared the properties of the clouds moving in elongated orbits along the Galactic bar with the better known clouds of the Galactic center ring (GCR). The gas of the GCR is dense, warm and exhibits a rich chemistry. The UV radiation can only account for the heating of 10-30 % of the warm gas. The rest of the warm gas can be heated by C-shocks if the magnetic field intensity is higher than 300 μ G. The high abundance of molecules linked to the grain chemistry also points to the presence of shock waves. A recent survey has shown that all the kinematical components of the Galactic center contain dense clouds that can withstand the tidal shear. This includes the structures with non-circular velocities like the dust lanes along the bar. However, in the GC there are no signs of star formation except in the nuclear ring (the GCR). The high relative velocities and shear expected in other kinematical structures, in particular in those associated with the dust lanes, could inhibit the star formation. The high measured abundances of one of the most representative molecules of the GC shock chemistry (SiO) in the cloud components associated with the dust lanes can be due to the large scale shocks that created the structures themselves.

References

- [1] Athanassoula, E. 1992, MNRAS, 259, 345
- [2] Bachiller, R. & Perez Gutierrez, M. 1997, ApJ, 487, L93
- [3] Bally, J., Stark, A. A., Wilson, R. W., & Henkel, C. 1987, ApJS, 65, 13
- [4] Binney, J., Gerhard, O. E., Stark, A. A., Bally, J., & Uchida, K. I. 1991, MNRAS, 252, 210
- [5] Bitran, M., Alvarez, H., Bronfman, L., May, J., & Thaddeus, P. 1997, A&AS, 125, 99
- [6] Cabrit, S., Lefloch, B., Cernicharo, J., Pineau Des Forêts, G., Lebourlot, J., & Flower, D. 2004, The Dense Interstellar Medium in Galaxies, 587
- [7] Dahmen, G., Huettemeister, S., Wilson, T. L., Mauersberger, R., Linhart, A., Bronfman, L., Tieftrunk, A. R., Meyer, K., Wiedenhoefer, W., Dame, T. M., Palmer, E. S., May, J., Aparici, J., & Mac-Auliffe, F. 1997, A&AS, 126, 197
- [8] Fux, R. 1999, A&A, 345, 787
- [9] Greaves, J. S., Ohishi, M., & Nyman, L.-A. 1996, A&A, 307, 898
- [10] Güsten, R. 1989, in IAU Symp. 136: The Center of the Galaxy, ed M. Morris, 89
- [11] Hüttemeister, S., Dahmen, G., Mauersberger, R., Henkel, C., Wilson, T. L., & Martin-Pintado, J. 1998, A&A, 334, 646
- [12] Hüttemeister, S., Wilson, T. L., Bania, T. M., & Martin-Pintado, J. 1993, A&A, 280, 255
- [13] Jackson, J. M., Heyer, M. H., Paglione, T. A. D., & Bolatto, A. D. 1996, ApJ, 456, L91+
- [14] Lis, D. C., Serabyn, E., Zylka, R., & Li, Y. 2001, ApJ, 550, 761
- [15] Lucas, R. & Liszt, H. S. 2000, A&A, 355, 327
- [16] Martin, C. L., Walsh, W. M., Xiao, K., Lane, A. P., Walker, C. K., & Stark, A. A. 2004, ApJS, 150, 239
- [17] Martin-Pintado, J., Bachiller, R., & Fuente, A. 1992, A&A, 254, 315
- [18] Martín-Pintado, J., de Vicente, P., Fuente, A., & Planesas, P. 1997, ApJ, 482, L45
- [19] Martín-Pintado, J., de Vicente, P., Rodríguez-Fernández, N. J., Fuente, A., & Planesas, P. 2000, A&A, 356, L5
- [20] Martín-Pintado, J., Gaume, R. A., Rodríguez-Fernández, N., de Vicente, P., & Wilson, T. L. 1999, ApJ, 519, 667
- [21] Martín-Pintado, J., Rizzo, J. R., de Vicente, P., Rodríguez-Fernández, N. J., & Fuente, A. 2001, ApJ, 548, L65

- [22] Meier, D. S. & Turner, J. L. 2005, *ApJ*, 618, 259
- [23] Morris, M., & Serabyn, E. 1996, *ARA&A*, 34, 645
- [24] Oka, T., Hasegawa, T., Hayashi, M., Handa, T., & Sakamoto, S. 1998a, *ApJ*, 493, 730
- [25] Requena-Torres, M. A., Martín-Pintado, J., Rodríguez-Franco, A., Martín, S., Rodríguez-Fernández, N. J., & de Vicente, P. 2006, *ArXiv Astrophysics e-prints*, arXiv:astro-ph/0605031
- [26] Reynaud, D. & Downes, D. 1998, *A&A*, 337, 671
- [27] Rodríguez-Fernández, N. J., Martín-Pintado, J., de Vicente, P., Fuente, A., Hüttemeister, S., Wilson, T. L., & Kunze, D. 2000, *A&A*, 356, 695
- [28] Rodríguez-Fernández, N. J., Martín-Pintado, J., Fuente, A., de Vicente, P., Wilson, T. L., & Hüttemeister, S. 2001, *A&A*, 365, 174
- [29] Rodríguez-Fernández, N. J., Martín-Pintado, J., de Vicente, P. 2001, *A&A*, 377, 631
- [30] Rodríguez-Fernández, N. J., Martín-Pintado, J., Fuente, A., & Wilson, T. L. 2004, *A&A*, 427, 217
- [31] Rodríguez-Fernández, N. J., Martín-Pintado, J., 2005, *A&A*, 429, 923
- [32] Rodríguez-Fernández, N., Combes, F., Martín-Pintado, J., Wilson, T. L., & Apponi, A. 2006, *ArXiv Astrophysics e-prints*, arXiv:astro-ph/0603851
- [33] Sato, F., Hasegawa, T., Whiteoak, J. B., & Miyawaki, R. 2000, *ApJ*, 535, 857
- [34] Sawada, T., Hasegawa, T., Handa, T., Morino, J.-I., Oka, T., Booth, R., Bronfman, L., Hayashi, M., Luna Castellanos, A., Nyman, L.-Å., Sakamoto, S., Seta, M., Shaver, P., Sorai, K., & Usuda, K. S. 2001, *ApJS*, 136, 189
- [35] Schilke, P., Pineau des Forêts, G., Walmsley, C. M., & Martín-Pintado, J. 2001, *A&A*, 372, 291
- [36] Schilke, P., Walmsley, C. M., Pineau des Forêts, G., & Flower, D. R. 1997, *A&A*, 321, 293
- [37] Sheth, K., Regan, M. W., Vogel, S. N., & Teuben, P. J. 2000, *ApJ*, 532, 221
- [38] Stark, A. A., Martin, C. L., Walsh, W. M., Xiao, K., Lane, A. P., & Walker, C. K. 2004, *ApJ*, 614, L41
- [39] Tsuboi, M., Handa, T., & Ukita, N. 1999, *ApJS*, 120, 1
- [40] Tubbs, A. D. 1982, *ApJ*, 255, 458
- [41] Usero, A., García-Burillo, S., Martín-Pintado, J., Fuente, A., & Neri, R. 2005, *ArXiv Astrophysics e-prints*
- [42] Wilson, T. L., Ruf, K., Walmsley, C. M., Martin, R. N., Batrla, W., & Pauls, T. A. 1982, *A&A*, 115, 185
- [43] Ziurys, L. M., Friberg, P., & Irvine, W. M. 1989, *ApJ*, 343, 201